Original Research Article

SACRED HEART RESEARCH PUBLICATIONS

Journal of Functional Materials and Biomolecules

Journal homepage: www.shcpub.edu.in

ISSN: 2456-9429

Exploration of Growth, Characterization and Hirshfeld Analysis of Benzimidazolium *l*- Aspartate for optoelectronic applications

Sudha N[a], Janani S[a*], Mathammal R[a], Gayathri P[a]

Received on 28 March 2020, accepted on 10 July 2020,
Published online on 17 July 2020

Abstract

Organic nonlinear optical crystal Benzimidazolium-L-aspartate (BLA) was successfully grown at room temperature from its aqueous solution by slow evaporation technique. The cell parameters of the grown crystal were found by Single X-ray Diffraction and it belongs to monoclinic system with space group $P2_1/c$. The intermolecular interactions were identified by Hirshfeld surface analysis. The presence of functional groups in the grown crystal was identified by FT-IR analysis. The optical transmittance and the lower cut-off wavelength of the grown crystal have been identified by UV-Vis study. The electronic structure of materials is examined using the technique of Photoluminescence spectroscopy. The dielectric constant and dielectric loss of the crystal was also studied as a function of frequency. Mechanical strength was found by Vicker's micro hardness test. The Second Harmonic Generation efficiency was measured in comparison with urea by employing Kurtz – Perry powder technique. antimicrobial compounds to treat the diseases.

Keywords: Crystal Growth, XRD, Hirshfeld, FTIR, UV, SHG.

1 Introduction

In recent years, organic nonlinear optical crystals are greatly investigated due to their high nonlinearities and rapid response in electro-optic effect compared to inorganic materials. The organic materials have strong nonlinear optical properties due to the presence of delocalized π electron system having donor and acceptor groups enhancing the asymmetric polarizability. In the organic nonlinear optical crystals may also play an important role in electro-optic modulation, frequency mixing, second harmonic generation, optical parametric oscillation, etc [1, 2]. Crystal growth from solution is an important process that is used in many applications from laboratory to industrial scale. An innumerable number of organic and inorganic crystals are grown in this fashion [3]. Benzimidazoles are involved in a great variety of biological processes and proved to possess antibacterial, fungicide and antihelmintic activity [4, 5]. Benzimidazole and its derivatives promote intra and inter-molecular interactions, such as hydrogen bonding and π – stacking giving place to the formation of molecular aggregates [6].

Benzimidazole compounds are of great interest especially in the synthesis of NLO materials which can be used in the fabrication of optoelectronic and photonic devices. The structure and properties of aspartic acid complexes like L-Lysine-L-Aspartate, Histindinium-L-Aspartate, Arginine-L-Aspartate, have been already reported [7-10]. The structure of Benzimiazolium L-aspartate (BLA) is already reported by Amudha et al [11]. The Benzimidazole molecule is protonated forming a Benzimidazolium molecule and the L- aspartic acid molecule undergone deprotonation and also transferred the other carboxylic acid proton to the amine group. In the present work, BLA crystals were grown by slow evaporation growth technique subjected to various characterization to be used for industrial applications. The grown crystals were subjected to single crystal X-ray diffraction analysis, Hirshfeld analysis, FT-IR, UV-Vis, Photoluminescence studies, micro hardness and dielectric studies. The NLO property of the grown crystal has been confirmed by Kurtz-Perry SHG test.

2 Experimental

2.1 Material synthesis

Fig1. Photo of as grown BLA crystal.

*Corresponding author: e-mail s.jananiphysics@gmail.com
[a]Department of Physics, Sri Sarada College for Women (Autonomous) Salem-16, Tamil Nadu, India.

BLA crystal was synthesized by dissolving benzimidazole and L-aspartic acid in ethanol in equimolar ratio (1:1) and the resulting solution was stirred well for about 4 hours and clear solution was obtained. The solution was filtered using whatmann filter paper. In a clean vessel the solution was closed with filter paper and maintained at room temperature without disturbance. In about 14 days, good transparent quality, colorless crystals were harvested. The size of the grown crystal is 4x2x2 mm^3. The photograph of BLA crystal is shown in Fig1.

3 Results and Discussion

3.1 Single crystal X-ray diffraction

The cell parameters of BLA crystal were estimated by single crystal X-ray diffraction analysis and the cell parameters are a=8.8513 Å, b=5.0232 Å, c=12.5075 Å and α = 89.95°, β=100.11°, γ=90°. The grown crystal belongs to monoclinic crystal system with space group P21/c. The volume of the system is V=541.32 $Å^3$. The single crystal XRD data determined in the present work for BLA was found to be in good agreement with the reported values [11]. The crystal data of BLA crystal is given in Table 1.

Table: 1 Single crystal data of BLA crystal.

Lattice parameters	Present work	Reported work
a (A°)	8.8513	8.9612
b(A°)	5.0232	5.0796
c(A°)	12.5075	12.5535
α (deg)	89.95	90
β(deg)	100.11	102.4380
δ(deg)	90	90
V $Å^3$	541.32	558.02
System	Monoclinic	Monoclinic
Space group	P21/c	P21/c

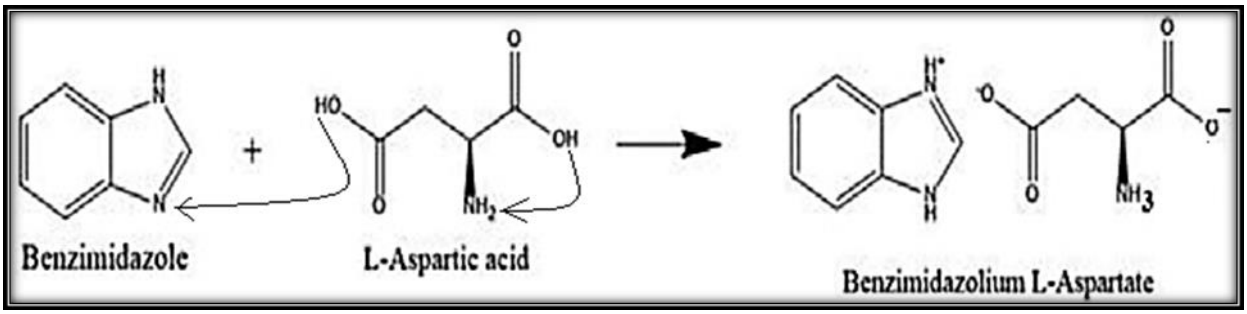

Fig 2. Reaction mechanism of BLA

During the chemical reaction between Benzimidazole and *l*- aspartic acid is shown in Fig 2. A proton from one end of acid moves to the nitrogen of the Benzimidazole forming a salt. As well as proton from another end of acid moves to the NH_2 of the same molecule forms a zwitterion. In the cation of the title molecular salt, $C_7H_7N_2^+.C_4H_6NO_4^-$ (systematic name: 1H-benzo[d]imidazol-3-ium 2-azaniumylsuccinate), the benzimidazole ring system is almost planar (r.m.s. deviation =0.012Å). The cation is protonated at the N atom and the L-aspartate zwitterions is deprotonated at both carboxyl groups. In the anion, an N-H…O hydrogen bond and an N-H…O short contact generate S (6) graph-set motifs. In the crystal, the anions are linked *via* three N-H…O hydrogen bonds involving the NH_3^+ group, forming layers parallel to the *ab* plane. The benzimidazolium cations are linked to these layers by N-H…O hydrogen bonds. The layers are linked *via* C-H…O hydrogen bonds involving the benzimidazolium cation, forming a three-dimensional structure. There is also C-H…π interactions present involving inversion-related benzimidazolium cations [12].

3.2 Hirshfeld surface analysis

A Hirshfeld surface analysis [13] was performed to visualize the different types of interactions present with in a crystal structure using the crystal Explorer 3.1 software [14], which accepts a structure input file in the Crystallographic Information File (CIF) format. Hirshfeld surfaces are produced through the partitioning of space within a crystal where the ratio of promolecule to procrystal electron densities is equal to 0.5 and are mapped using the Normalized contact distance (dnorm) which is defined in terms of external and internal distances de and di and the van der Waals (vdW) radii of atoms.

In the crystal structure, intermolecular interactions were analyzed for the asymmetric unit using the 3D Hirshfeld surfaces Fig 3a and 2D fingerprint maps Fig 4 .The dnorm values are mapped onto the Hirshfeld surface by using a red-blue-white color scheme: red regions represent closer contacts and negative dnorm value; blue regions representant longer contacts and positive dnorm value; and white regions represent the distance of contacts is exactly the vdW separation and with a dnorm value of zero. The shape index is the most sensitive to changes in surface shape, the information conveyed by shape index are consisted with the 2D fingerprint plots. Hirshfeld surfaces mapped over the shape index of BLA are shown in Fig 3b. The 2D fingerprint plots can be decomposed to highlight particular atom pair close contacts [15-17].

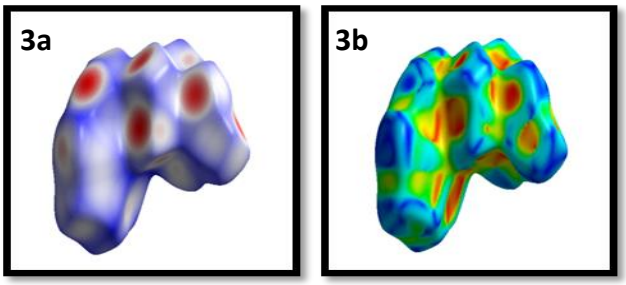

Fig 3. Hirshfeld surface with d_{norm} and shape index

The contributions from different interaction types which overlap in the full fingerprint (100%) are then separated Fig 4a. The highest contribution occur due to O…H contact 24.5 % (d_i =2.530 Å, d_e =0.450 Å) Fig 4b. The H…O interactions are represented by a small area in the top left side of the fingerprint plot and their contribution reaches 21.6% (d_i= 2.495 Å, d_e =0.490 Å) Fig 4c. The C…H interactions are represented by a spike in the bottom right region of fingerprint plot and their relative contact 9.6% (d_i=2.490 Å, d_e=0.520 Å) Fig 4d. The fingerprint plot shows that H…C contacts comprise 6.9% (d_i=2.555 Å d_e=0.575 Å) Fig 4e. Lower percentages are observed for bottom right side of the interaction N…H contact 1.8% (d_i=2.545 Å, d_e=0.495 Å) Fig 4f and the top right side of the fingerprint plot H…N contact1.2%(d_i=2.460 Å, d_e=0.470 Å) Fig 4g. The O…H/H…O interactions has the most participation in the crystal structures.

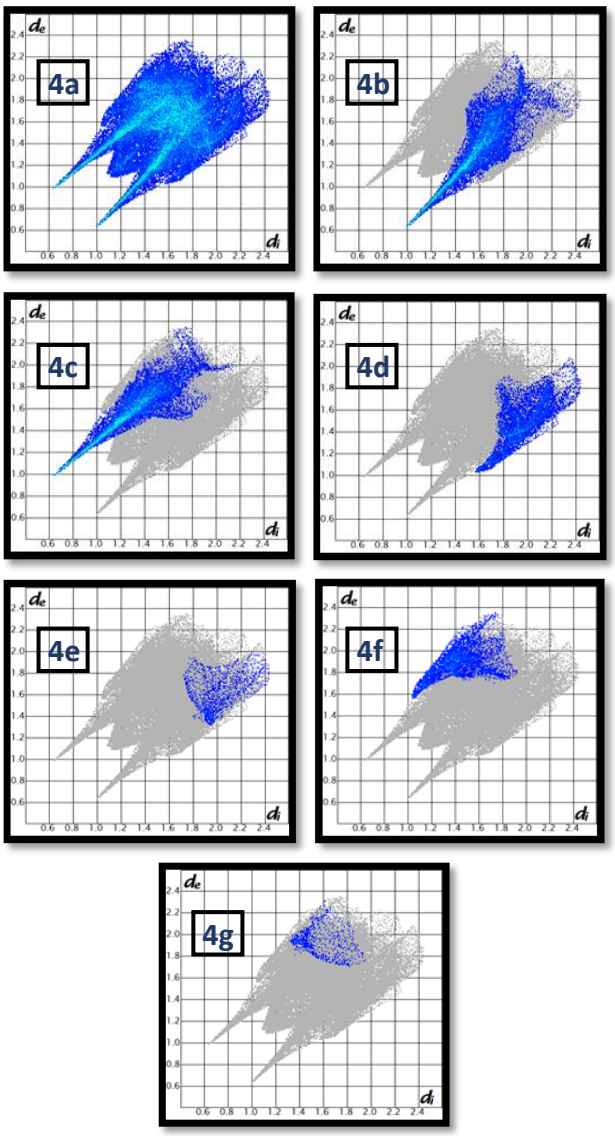

Fig 4. 2D fingerprint plots of the title complex where areas of different intermolecular contacts are clearly shown; d_e and d_i are the distances to the nearest atom exterior and interior to the surface.

3.3 FT-IR spectral analysis

The functional groups were identified by Fourier transform infrared studies using (PERKIN ELMER) spectrometer. The FTIR spectrum of BLA was recorded in the range of 4000 to 400 cm^{-1} as shown in Fig 5. The C-H stretching in a ring is generally observed between 3100-3000 cm^{-1}. In the present compound C-H stretching vibration is evident by the peaks at 3063, 3039, 3005 cm^{-1} [18]. The general wavelength of C=O stretching vibration is observed between 1850-1690 cm^{-1}. In the present case the peak at 1772 cm^{-1} is due to C=O stretching vibration. The general wavelength of C=N stretching vibration is observed between 1650-1580cm^{-1}. In the title molecule peak at 1619 cm^{-1}. The general wavelength of ring vibrations is observed between 1650-1430 cm^{-1} in the present case intense peaks at 1587, 1477, 1458, 1409 cm^{-1} are due to ring vibrations [18]. The general value of C-O stretching vibration is observed between 1370-1210cm^{-1}. In the present case peaks at 1363, 1272 cm^{-1} are due to C-O stretching vibration. The general value of C-N stretching vibration is observed between 1600-1030cm^{-1}. The peaks at 1246 cm^{-1} is assigned due to C-N stretching vibration. The general value of O-H bending is observed between 1400-920 cm^{-1}. In the present case peaks at 1002 cm^{-1} and 956 cm^{-1} in which both spectrums are assigned to the O-H bending. The general value of COO^- rocking is observed between 900-550 cm^{-1}. Whereas peak at 578 cm^{-1} has assigned to COO^- rocking [29]. The vibrational assignments are shown Table 2.

Table 2. FTIR assignments of BLA crystal.

Wave number in (cm^{-1})	Assignment of vibration
3063, 3039, 3005	C-H stretching vibration
1772	C=O stretching vibration
1619	C=N stretching vibration
1587.56, 1477, 1458, 1409	ring vibrations
1363, 1272	C-O stretching vibration
1246	C-N stretching vibration
1002 ,956	O-H bending
578	COO^- rocking

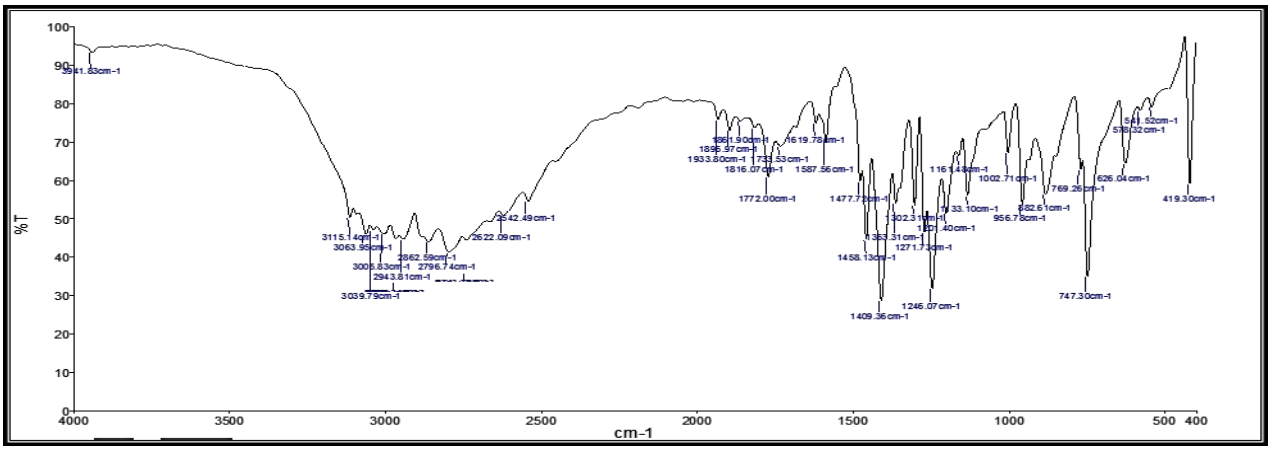

Fig 5. FT-IR spectrum of BLA crystal

3.4 UV-Vis spectral analysis

Good optical transmittance and lower cutoff wavelengths are very important properties for NLO crystals [20]. The absorption spectrum of BLA crystal was recorded in the wavelength range between 200 to 1100 nm using UV-Vis Perkin Elmer model: lambda 35 spectrometer. The absorption spectrum is shown in Fig 6a. The transmission spectrum is one of the important factor to identify NLO materials. The crystal is transparent from 277to 1100 nm which proves that there is no absorption in most of the visible region, the wide transparency in the visible region proves that BLA crystal is a potential candidate for optical applications. The transmission spectrum is shown in Fig 6b.

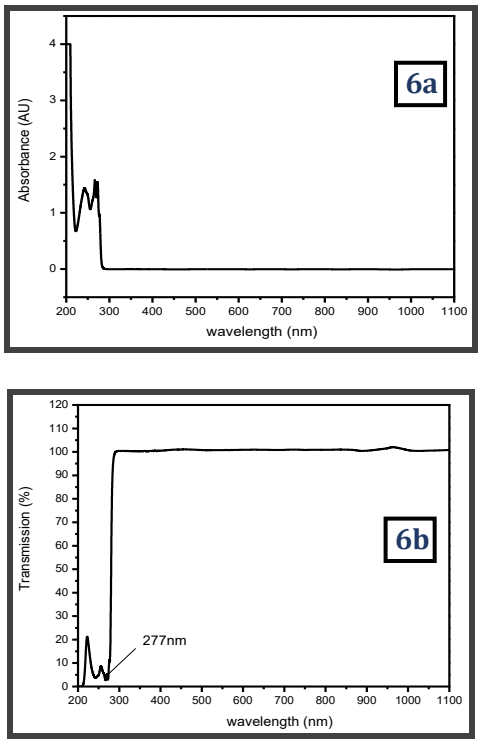

Fig 6a. and 6b. Plot of absorbance and transmission spectrum of BLA crystal

The band gap (E_g) can be evaluated from the transmission spectra [21]. Energy gap of BLA is calculated by using the formula,

$$E_g = 1243/\lambda$$
$$=1243/277 = 4.48 \text{ eV}$$

λ is lower cut-off wavelength and the band gap of BLA was found to be 4.48 eV.

3.5 Photoluminescence studies

Photoluminescence is the spontaneous emission of light from a material under optical excitation. PL investigations can be used to characterize a variety of material parameter. This spectrum was recorded using Perkin Elmer LS 45 luminescence spectrometer. The emission spectrum was recorded in the range of 260 to 500 nm. The emission spectrum is shown in Fig 7. A broad emission band observed in the range 292 nm indicates that BLA crystal has a violet fluorescence emission. So, it can be used in the fabrication of optoelectronic and photonic devices.

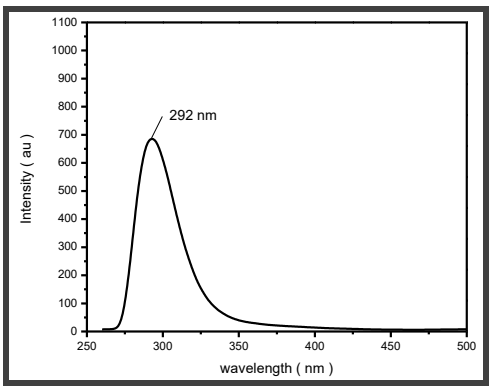

Fig 7. Plot of Photoluminescence spectrum of BLA crystal.

3.6 Microhardness studies

Hardness test are commonly used to determine the mechanical strength of the grown crystal. BLA was tested

for their micro hardness property using shimadzu model 27. Vickers's micro hardness tested fitted with a diamond in denter selected smooth and flat surfaces of the grown crystal were subjected to this study. The measurements were made at room temperature and loads of different magnitude such as 25, 50 and 100 g were applied [22]. The Vicker`s hardness number (H_v) is calculated using the formula [23],

$$H_v = 1.8544\ p/d^2\ kg/mm^2$$

Where, p is the applied load in kg and d is the diagonal length in mm. 1.8544 is a constant of geometrical factor for the diamond pyramid.

The variation of Hv with the applied load is shown in Fig 8. From the plot it is found that on increasing the load the hardness increases. A plot obtained between log (p) and log (d) gives more or less straight line which is shown in Fig 9.

The relation connecting the applied load (p) and diagonal length (d) of the indenter is given by Meyer's law, $p = ad^n$ [24].

Here n is Meyer's index or work hardening coefficient that has been calculated from the slope of the straight line. According to Onitsch and Hanneman [25] pointed out that n lies between 1 and 1.6 for hard material and more than 1.6 for soft material. The slope of the graph gives n value and it was found to be 2. Hence, it is concluded that BLA crystal belongs to the soft material category.

3.7 Dielectric studies

The dielectric properties of the optical crystals are well associated with electro – optic properties particularly for non-conducting crystals [26]. The dielectric constant is one of the basic electrical properties of solids [27].

The dielectric constant was calculated by using the relation,

$$\varepsilon_r = c\ d/\varepsilon_0 A$$

Where, C is the capacitance, d is the thickness of the crystal, $\varepsilon_0$is the permittivity of free space and A is the area of the crystal.

The high values of dielectric constant at low frequencies may be due to presences of space charge, orientation, ionic and electronic polarizations and it is depending on the frequencies [28-30]. The higher value of dielectric constant with lower frequencies may be attributed to space charge and polarizations enhance second harmonic generation [31].

Fig 10, shows the variation of dielectric constant with frequency at room temperature. This is normal dielectric behavior that both dielectric constant and dielectric loss decrease with an increase in frequency. The variation of dielectric loss tan δ with frequencies is shown in Fig 11. The value of dielectric loss at high frequency reveals the high optical quality of the crystal with lesser defects and this is a desirable property for NLO applications [32].

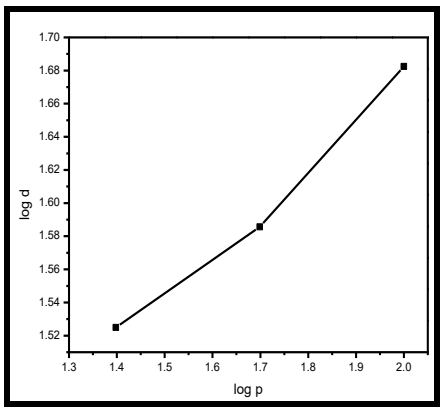

Fig 8. Plot between Hv and load p

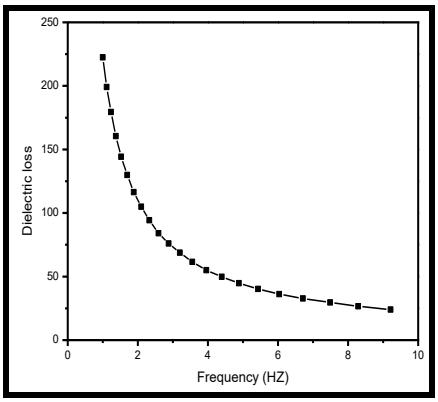

Fig 10. Plot of dielectric constant V_s frequency.

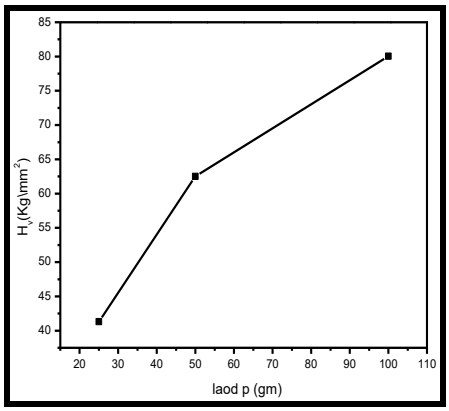

Fig 9. Plot between log p and log d

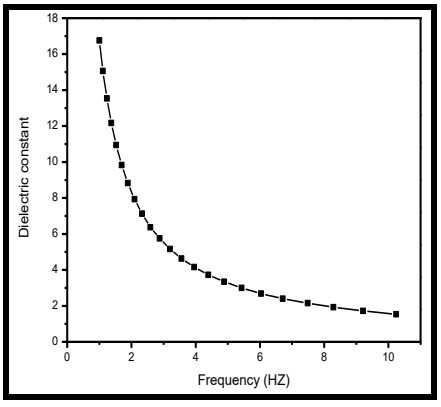

Fig 11. Plot of dielectric loss V_s frequency.

3.8 NLO Second Harmonic Generation

The Second Harmonic Generation behavior of BLA was analyzed by a modified version of the powder technique developed by Kurtz and Perry [33]. The crystal was illuminated using Q- switched Nd: YAG laser using the fundamental beam of 1064 nm with a pulse width of 8 ns with a repetition rate of 10 Hz was used. The incident input energy of 1.2mJ/pulse was incident on the crystalline powder, which filled in the micro capillary tube. The second harmonic signal generated in the crystal was confirmed from the emission of green radiation of wavelength 532 nm. Hence it is observed that the SHG efficiency of BLA is 0.3 times that of urea proving that BLA is a suitable candidate for NLO applications [34].

4 Conclusions

Good optical quality Benzimidazolium *l*-aspartate was grown by slow evaporation solution growth method at room temperature. Single crystal XRD analysis confirmed that the BLA crystal belongs to the monoclinic system with space group $P2_1/c$. The 3D Hirshfeld surface analysis and 2D fingerprint maps analysis revealed that O…H/H…O and C…H/H…C hydrogen bonding intermolecular interactions are more prominent in the salt. The FT-IR spectrum reveals that the various functional groups present in the crystal. The lower cut- off wavelength (277 nm) and the transmittance (277 to 1100 nm) from the UV-Vis spectral studies and the optical band gap energy is found to be 4.48 eV. The violet emission occurred at 292nm in Photoluminescence studies. Micro hardness studies confirmed that the grown crystal belongs to soft material category. The dielectric studies prove that the sample has low dielectric constant and dielectric loss values at high frequency. The powder SHG efficiency analysis reveals that the efficiency of this crystal is about 0.33 times that of urea. All these results propose the crystal as a potential candidate for NLO applications.

Acknowledgements

The authors acknowledge SAIF for Single XRD and St. Joseph College in Tirchy for providing UV-Vis, FT-IR, Dielectric and Hardness studies. IISC Bangalore for SHG measurements and Sri Sarada College for Women (Autonomous) Salem -16 for facilitating my research work.

Conflict of Interest:

All authors have no conflict of interest to report.

References

[1] D.S.Chemla, J.Zyss, nonlinear optical properties of Organic Molecules and crystal, Vol.1, Academic press, London, 1987.

[2] J.Badan, R.Hierle, A.Perigand, J.zyss, in: Williams (Ed.), Nonlinear Optical properties of Organic molecules and polymeric Materials,vol.233, Am. Chem. Soc., Washington, DC, 1993,P,D5.

[3] S.A. deVries, P. Goedtkind, W.J.Huisman, M.J. Zwanenburg, R.Feidenhans' 1, S.L.Bennett, D.M. Smilgies, A. Stierle, J.J. De Yoreo, W.J.P. Van Enckevort, P.Bennema, E.Vlieg, J. Crystal growth 205 (1999) 202.

[4] N.S. Pawar, D.S. Dalal, S.R. Shimpi, & P.P. Mahulikar, (2004). Eur. J. Pharm. Sci., 21,115.

[5] Oren. I, Temiz. O, Yalcin I., Sener. E,&Altanlar. N. (1998). Eur.J.Pharm.sci., 7, 153.3.

[6] A. Chandramohan, R.Bharathikannan, M. A. Kandhaswamy, J. Chandrasekaran, R. Renganathan, & V. Kandhavelu, (2008). Cryst. Res.Technol., 43, 173.

[7] T.N. Bhat, &Vijayan, M.(1982). Acta Cryst.B32, 891-895.

[8] D.M. Salunke, &Vijayan, M.(1982). Actacryst, B38, 1328-1330.

[9] J. Soman, &Vijayan, M.(1988).ActaCryst., C44, 1794-1797.

[10] T.N.Bhat, &Vijayan, M.(1978). Actacryst. B34, 2556-2565.

[11] M. Amudha, A. Thirugnanam, K.Krishnaraj&P.PraveenkumarJ.Molecular crystals and liquid crystal650 (2017), 125-137.

[12] M. Amudha, P. Praveen kumar and G.ChakkaravarthiIUCr Data (2016). 1. x160677.

[13] J.J. Mckinnon, D.Jayatilaka, M.A. Spackman, Chemcommun, (2007) 3814-3816.

[14] S.K. Wolff, D.J. Grimwood, J.J. Mckinnon, M.J. Turner, D. Jayatilaka, M.A Speckman, Crystal-explorer 3.1, university of western Australia, Perth, 2012.

[15] H.Khanam, A.Mashrai, N. Siddiqui, M.Ahmad, M.J. Alam, S.Ahmed, Shamsuzzaman, J. Mol. Struct. 1084 (2015) 274-283.

[16] Y.H. Ma, S.W. Ge, W.Wang, B.W. Sun, J. Mol.struct. 1097 (2015) 87-97.

[17] S. Madan Kumar, B.C. Manjunath, G.S. Lingaraju, M.M.M.Abdon, M.P. Sadashve, N.K. Lokanath, Cryst.struct. Theory Appl. 2 (2013) 124-131.

[18] N. Vijayan, R. Ramesh Babu, R. Gopalakrishnan, P. Ramasamy, W.T.A. Harrison. Crystal growth 262 (2004) 490-498.

[19] SwetaMoitra, Saikat Seth, TanusreKar. J. growth 312 (2010) 1977-1982.

[20] T. Balakrishnan, k. Ramamurthy, spectrochim Act a part A, 72(2009) 269-273.

[21] A .Ashour, N . El-Kadry, S.A. Mahmud , Thin solid Films 1995; 267: 117-209.

[22] N. Sudharsana, B. keerthana, R. Nagalakshmi, Materials chemistry and physics 134 (2012) 736-746.

[23] B.W.Mott, micro indentation hardness testing, Butterworths, London, 1956.
[24] Mayer, some aspects of the hardness of metals, ph.D. Thesis, dreft, 1951.
[25] E.M. Onitsch, Microscopy 2(1947) 131.
[26] S. Boomadevi, R. Dhanaskaran, J. cryst. Growth 261, 70 (2004).
[27] P. V.Dhanraj, N.P.Rajesh, C.K. Mahadevan, G. Bhagavannarayana, phy B 404 (2009) 2503-2508.
[28] K.V Rao, A. Samakula, J.Appl. phys. 36 (1965) 2031.
[29] P. Selvarajan, B. N .Das, H.B. Gon, K. V Rao, J. Master. Sci. 29(1994) 4061.
[30] N. V. Prasad, G.Prasad, T.Bhimasakaran, S.V. Suryanarayana, G.S. Kumar, Indian J. pure Appl, phys 34 (1996) 639.
[31] I. G. Austin, N.F. Mutt, Adv, phys, 18 (1969) 41-102.
[32] C. Balarew, R. Duhlew, J. Solid state chem. 55 (1984) 1-6.
[33] S.K.Kurtz, T.T Perry J.Appl.phys.39 (1968) 3798.
[34] T.P Srinivasan et al/ J. cryst .growth 312 (2010) 542-547.